International Journal of Greenhouse Gas Control 39 (2015) 17–26

International Journal of Greenhouse Gas Control

journal homepage: www.elsevier.com/locate/ijggc

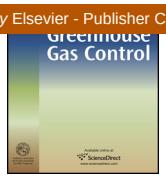

Process simulation of a dual-stage Selexol process for 95% carbon capture efficiency at an integrated gasification combined cycle power plant

Zoe Kapetaki, Pietro Brandani, Stefano Brandani, Hyungwoong Ahn *

Scottish Carbon Capture and Storage Centre, Institute for Materials and Processes, School of Engineering, The University of Edinburgh, Mayfield Road, Edinburgh, EH9 3JL, UK

ARTICLE INFO

Article history:
Received 1 December 2014
Received in revised form 11 March 2015
Accepted 23 April 2015
Available online 15 May 2015

Keywords:
Selexol
Dual-stage Selexol process
Process simulation
Integrated gasification combined cycle
Carbon capture

ABSTRACT

It was aimed to simulate a conventional dual-stage Selexol process for removing CO_2 and H_2S simultaneously from a synthesis gas (syngas) originated from a typical Integrated Gasification Combined Cycle (IGCC) power plant driven by a dry-coal fed gasifier using Honeywell UniSim R400. The solubilities of syngas components on Selexol were predicted by temperature-dependant Henry's law constants being newly evaluated in this study based on the experimental data in Xu et al. (1992). The operating conditions of the dual-stage Selexol unit were determined so as to meet simultaneously various performance targets, such as 99+% H_2 recovery, 90% CO_2 recovery, 99+% H_2S recovery, and less than 20 ppm H_2S in CO_2 product. By and large the resulting energy consumptions of the Selexol process were in good agreement with those reported in DOE NETL (2010) that this study was based on. It was shown that the integrated dual-stage Selexol unit could achieve 95% carbon capture rate as well as 90% by simply changing the operating conditions. By contrast a CO_2 removal Selexol process having not an input of lean solvent generated by thermal regeneration could not achieve 95% carbon capture rate due to a pinch point formed at the top of the CO_2 absorber.

1. Introduction

Anthropogenic CO_2 emissions into the air have long been thought to be the most important agent to give rise to global warming and climate change. Carbon capture and storage must be one of the most efficient and practical ways of curtailing the amount of CO_2 being emitted into the air in the near future. Capturing CO_2 from other industries cannot be more important than decarbonising power sectors since power sectors accounts for more than 30% of the total UK anthropogenic CO_2 emission (Committee on Climate Change, 2013). Integrated Gasification Combined Cycle (IGCC) power plants have been considered as the most advanced fossil fuel-based power generation technologies due to their greater net power efficiencies than those of conventional PC-fired boiler power plants (DOE NETL, 2010). In addition to their outstanding power efficiencies, IGCCs are deemed as more environment-friendly than PC-fired boiler power plants since contaminants can be removed at less cost (Rubin et al., 2007; Chen and Rubin 2009). In IGCC, the sulfur species contained in a coal can be removed from the syngas stream using an acid gas removal process before the fuel is combusted. The acid gas removal unit for H_2S removal in IGCCs can operate at a higher pressure and with a less volumetric gas flow than the Flue Gas Desulphurisation (FGD) unit for SO_2 removal in PC-fired boiler power plants being applied to the flue gas after combustion.

The advantage of IGCCs being capable of removing sulfurs economically over PC-fired boiler power plants is also exploitable for CO_2 removal. In other words, it is likely that, for capturing CO_2 from IGCCs, pre-combustion capture technologies could spend less energy than post-combustion capture technologies. The CO_2 partial pressure of a shifted syngas stream to which a pre-combustion carbon capture process is applied is in the range of 12–20 bar (DOE NETL, 2010) that is high enough to make use of physical solvents instead of chemical solvents for carbon capture. Up to now there have been extensive researches attempting to quantify energy consumptions in operating various physical absorption processes integrated with IGCCs and their associated net plant efficiencies as a result of integration. Doctor et al. (1996) evaluated several commercially available CO_2 capture technologies being incorporated into IGCC power plants for 90% carbon capture. Chiesa and Consonni

* Corresponding author. Tel.: +44 1316505891.
E-mail address: H.Ahn@ed.ac.uk (H. Ahn).

http://dx.doi.org/10.1016/j.ijggc.2015.04.015

(1999) studied a Selexol process to recover 90% CO_2 from a shifted syngas. They concluded that the addition of a Selexol process for carbon capture would result in 5–7% reduction in the LHV-based power efficiency and around 40% increase in the cost of electricity. DOE NETL (2002) investigated CO_2 capture from oxygen-blown, Destec and Shell-based IGCC power plants at the scale of a net electrical output of 400 MW_e. In the study, a dual-stage Selexol process was integrated for capturing CO_2 from IGCCs at an overall capture efficiency of 87%. O'Keefe et al. (2002) studied a 900 MW_e IGCC power plant integrated with a Selexol process for recovering 75% of the total carbon contained in the coal feed. Davison and Bressan (2003) compared the performances of several chemical or physical solvents including Selexol solvent for recovering 85% CO_2 from a coal-based 750 MW_e IGCC. Cormos and Agachi (2012) performed case studies on 400–500 MW_e net power IGCCs integrated with acid gas removal processes using several physical solvents including Selexol for 90–92 % carbon capture efficiency.

According to literature review on this subject, it is obvious that dual-stage Selexol processes have been recognised as the most conventional process for recovering H_2S and CO_2 simultaneously. This is because a Selexol solvent has (1) a very low vapour pressure to such an extent as to neglect solvent loss during process operation, (2) a good selectivity of H_2S over CO_2 that is crucial for dual-stage process configuration, and, most importantly, (3) a substantial CO_2 solubility. Selexol solvent has higher H_2 solubility than other commercial physical solvents, which may result in unsatisfactory H_2 recovery and excessive H_2 ingress into the CO_2 product. However the drawback can be overcome by a bespoke absorption process design featuring a solvent flash drum to recover H_2 from a CO_2-laden solvent. The flash drum for H_2 recovery has already been implemented in conventional CO_2 removal Selexol processes. For the design of acid gas removal processes using Selexol solvents, Kohl and Nielsen (1997) exhibited a simple two stage Selexol process composed of one set of absorber and steam stripper for H_2S removal followed by another set of absorber and air stripper for CO_2 removal. The simple two-stage Selexol process was simulated by Robinson and Luyben (2010). Bhattacharyya et al. (2011) implemented a comprehensive process simulation of an entire IGCC power plant integrated with a dual-stage Selexol process for 90% overall carbon capture efficiency. Padurean et al. (2012) reported an Aspen Plus simulation on a dual-stage Selexol unit at 70%, 80% and 90% CO_2 capture rate.

While most past researches have been devoted to Selexol process design for up to 90% carbon capture efficiency, this study presents process simulation results of dual-stage Selexol processes for achieving up to 95% carbon capture efficiency. In addition, it was attempted to clarify why dual-stage Selexol process must be designed to have the two H_2S and CO_2 absorbers integrated by sharing part of the circulating solvents. The power and thermal energy consumptions of various designs of dual-stage Selexol processes could be estimated accurately by performing their process simulation using a process flow sheeting simulator (UniSim R400).

2. Solubility model

It is essential that a process simulation for gas absorption and stripping be implemented on the basis of a reliable and robust solubility model. However, it is not easy to find a solubility model relevant to syngas absorption into Selexol. So far very few experimental data are available in the literature on the solubilities of syngas components in Selexol. This is because Selexol is neither a pure component nor a mixture of binary components unlike any other commercial physical solvents, such as methanol (Rectisol) and NMP (Purisol), but a mixture of various dimethyl ether of polyethylene glycol, $CH_3O(C_2H_4O)_nCH_3$ where n ranges from 2 to 9. Detailed information on Selexol composition has never been disclosed in the open literature to the best of our knowledge.

Basic physical properties of Selexol in UniSim were utilised in the process simulation without any modification. This is because the physical properties, such as molecular weight, density, heat capacity and so on, provided by UniSim as default are close to what were reported in literature (Burr and Lyddon, 2008; Kohl and Nielsen, 1997). Similarly the H_2S and CO_2 solubilities in Selexol provided by the UniSim library must be validated by their comparison with experimental data reported in the literature. Furthermore temperature dependency of gas solubilities need to be checked with experimental data since it is very likely that absorption and desorption of acid gases involves non-isothermal operation due to the heat of absorption.

To this end it is required to have Henry's constants measured experimentally at various temperatures. To the best of our knowledge, there is only one research paper reporting the effect of temperature on the solubilities of acid gases in Selexol (Xu et al., 1992). By contrast, other literature reported either Henry's constants or solubilities that were measured at a single temperature (Sweny and Valentine, 1970; Zhang et al., 1999; Confidential Company Research Report, 1979). It should be noted that Xu et al. (1992) measured the acid gas solubilities in a Selexol solvent in which small amount of water is contained. The water content of 0.87 wt% in Selexol apprears to be negligible in weight fraction but cannot be neglected in terms of molar fraction. This discrepancy is down to significant difference between the water and Selexol molecular weights. In this study, therefore, the Henry constants for H_2S and CO_2 in Selexol containing water reported in Xu et al. (1992) were corrected to those in pure, dehydrated Selexol assuming the CO_2 and H_2S solubilities in water would be negligible. In Fig. 1, the corrected Henry constants of CO_2 and H_2S in Selexol were plotted as a straight line.

However, the H_2S and CO_2 Henry constants in Selexol provided by UniSim library are both erroneously higher than those being corrected from Xu et al. (1992). As a result the H_2S and CO_2 solubilities predicted by the UniSim library underestimate significantly the corrected experimental solubilities as shown in Fig. 1. Therefore the default solubilities in UniSim cannot be used for the simulation of an acid gas removal Selexol process without modifying their Henry constants. Now that Xu et al. (1992) reported the temperature dependency of Henry constants, it was possible to estimate new temperature-dependent Henry constants based on their study. Henry's Law cannot be selected explicitly as a property method in UniSim Design but it can be used when an activity model is selected and non-condensable components such as syngas components of this study are included within the component list (UniSim Design, 2013). The correlation of Henry constant as a function of temperature in UniSim has the following formulae:

$$\ln K_i = A_i + \frac{B_i}{T} + C_i \ln(T) + D_i T \tag{1}$$

where K_i is the Henry constant of a component i [kPa], A_i is a constant and B_i to D_i are coefficients, and T is temperature [K]. Given the partial pressure of component i, p_i [kPa], the mole fraction of a solute in the liquid phase, x_i, can be expressed into $x_i = p_i / K_i$. But in this study, the presence of water must be taken into account in order to estimate the solubility of a solute in pure Selexol. For example, for estimating the CO_2 mole fraction in the liquid phase using the Henry constants reported in Xu et al. (1992), Eq. (2) was used.

$$X_{CO_2} = \frac{p_{CO_2}}{p_{CO_2} + (K_{CO_2} - p_{CO_2})\frac{n_{Selexol}}{n_{Solvent}}} \tag{2}$$

where $n_{Selexol} / n_{solvent}$ is the Selexol mole fraction in the solvent that is a mixture of Selexol and water. Corrected Henry constants

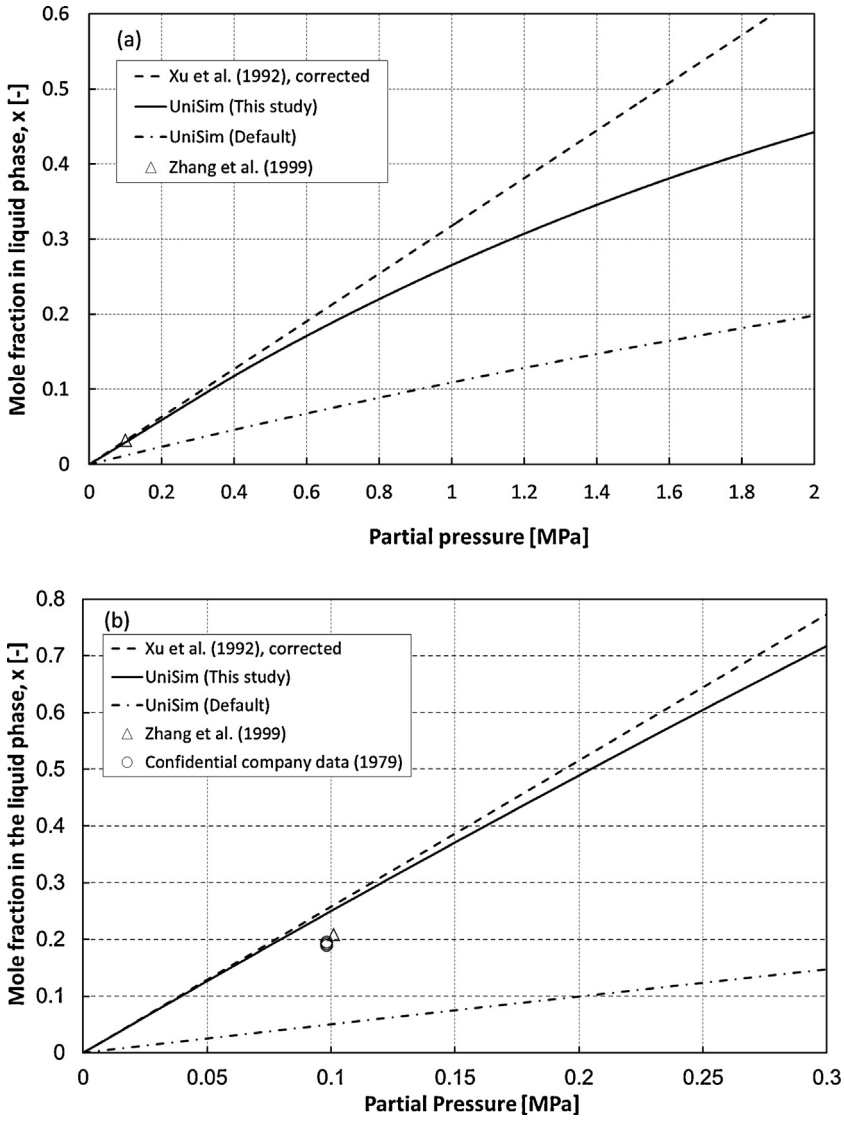

Fig. 1. Solubility of (a) CO_2 and (b) H_2S in Selexol at 298 K.

were in turn estimated using the mole fractions of CO_2 or H_2S in the liquid phase estimated by Eq. (2). The A_i and B_i in Eq. (1) correspond to the constant and coefficient of Van't Hoff equation, Eq. (3), respectively, with the other two coefficients, C_i and D_i, set to zero.

$$\ln K_i = \left(\frac{-\Delta H_i}{RT}\right) + \text{constant} \quad (3)$$

The A_i and B_i for each syngas component that were newly estimated in this study were used in Uni Sim instead of the defaults as listed in Table 1.

The Henry constants for CH_4, CO and N_2 were obtained on the basis of their solubility relative to CO_2 reported in the reference (Bucklin and Schendel, 1984; Burr and Lyddon, 2008) assuming the selectivity would be kept constant regardless of temperature. However temperature dependence of the Henry constant for H_2 in Selexol was neglected in marked contrast to those of the other components. It is well known that H_2 solubility in most hydrocarbon liquids increases with increasing temperature (Cai et al., 2001; Saajanlehto et al., 2014; Wang et al., 2013), indicating that the coefficient B_i in Eq. (1) for H_2 in Selexol is likely to be positive. Since the temperature dependence of H_2 solubility in Selexol could not be found in any literature, it was assumed that the known Henry constant for H_2 in Selexol at 25 °C on a basis of its solubility relative to CO_2 (Bucklin and Schendel, 1984) would not change within a restricted temperature range to be encountered in Selexol process operation. It was also assumed that Argon would act as an inert gas to Selexol solvent and water would be completely soluble with Selexol.

Fig. 1 also presents the solubilities of H_2S and CO_2 in Selexol estimated by UniSim using the constant and coefficient listed in Table 1. At a very low pressure, the UniSim estimations using the new set of A_i and B_i are capable of reproducing the corrected experimental solubilities of Xu et al. (1992). With the pressure increasing, the estimated solubilities deviate gradually from the straight lines of Henry's Law due to non-ideal behavior in the gas phase that was estimated by Peng–Robinson EOS.

The corrected experimental CO_2 solubility in Selexol (Xu et al., 1992) is in good agreement with the CO_2 solubility in Zhang et al. (1999). By contrast, the corrected H_2S solubility in Selexol was higher than the other two (Zhang et al., 1999; Confidential Company Research Report, 1979). This discrepancy implies that the H_2S solubility in Selexol used in this study may overestimate the actual H_2S solubility. However we decided to use the corrected experimental data based on Xu et al. (1992) in this study since the temperature dependency of the Henry constant for H_2S in Selexol

Table 1
The A_i and B_i of Eq. (1) for each gas component used in this study. (The two parameters for each gas except for H_2S and CO_2 were obtained on the basis of its solubility relative to CO_2 at 25 °C).

Component	A_i	B_i	Solubility of a gas in Selexol relative to CO_2 at 25 °C	
			Value	Reference
CO_2	13.828	−1720.0	1	–
H_2S	13.678	−2297.2	8.9	Bucklin and Schendel (1984)
H_2	12.402	0	$1.3{\cdot}10^{-2}$	Bucklin and Schendel (1984)
CH_4	16.531	−1720.0	$6.7{\cdot}10^{-2}$	Bucklin and Schendel (1984)
CO	17.403	−1720.0	$2.8{\cdot}10^{-2}$	Bucklin and Schendel (1984)
N_2	17.740	−1720.0	$2.0{\cdot}10^{-2}$	Burr and Lyddon (2008)

Table 2
Gas streams flowing to a Selexol process in this study (DOE Case 6, 2010).

Stream	(1) Main shifted syngas from mercury removal	(2) Recycle gas from Claus plant	(3) Gas feed flowing to Selexol unit (3 = 1 + 2)
Pressure [MPa]	3.59	5.51	3.59
Temperature [°C]	35	38	35
Molar flowrate [kmole/hr]	$2.884{\cdot}10^4$	400	$2.924{\cdot}10^4$
Mole fraction			
CO_2	0.3776	0.6257	0.3810
H_2S	0.0057	0.0057	0.0057
H_2	0.5633	0.2694	0.5593
CH_4	0.0004	0.0000	0.0004
CO	0.0084	0.0060	0.0084
H_2O	0.0016	0.0017	0.0016
N_2	0.0368	0.0813	0.0374
Ar	0.0062	0.0102	0.0062

was available only in their paper at the time of this study being implemented.

3. Conventional dual-stage Selexol process

A conventional dual-stage Selexol process for capturing H_2S and CO_2 from a syngas was simulated using the Honeywell UniSim R400 using a solubility model of the Henry's law using new sets of A_i and B_i listed in Table 1 in combination with vapor model correction using Peng–Robinson EOS. The temperature, pressure, gas composition and flowrate of a gas stream being fed to a dual-stage Selexol process were found in the reference (Case 6 of DOE NETL, 2010). The feed stream information was confirmed to be more or less correct by our independent process simulation (Kapetaki et al., 2013). As listed in Table 2, two different feed gas streams of (1) and (2) are combined to an actual gas feed, (3), being fed to Selexol process. One is a main syngas stream coming from a mercury removal unit downstream of a gasifier and the other is a recycle gas stream originating from a Claus plant. Following the reference study (DOE NETL, 2010), the carbon capture efficiency of an IGCC power plant integrated with a carbon capture unit is defined by Eq. (4).

$$\text{Carbon capture of efficiency} = \frac{\text{Carbon in } CO_2 \text{ product}}{\text{Carbon in coal feed} - \text{Carbon in slag}} \quad (4)$$

It should be noted that the carbon capture efficiency must be evaluated for all the carbon species contained in the CO_2 product inclusive of CO and CH_4 as well as CO_2. This is because Selexol is also capable of capturing CO and CH_4 even though their solubilities in Selexol are much less than the CO_2 solubility as shown in Table 1. According to the reference (Case 6 of DOE NETL, 2010), the total amount of carbon entering the IGCC power plant as a coal feed is 134,527 kg/hr and the carbon leaving the plant as a slag is 1483 kg/hr. The denominator of Eq. (4) was kept constant for all simulation cases of this study since our study was based on the constant flowrate of coal feed to an identical gasifier regardless of carbon capture integration.

The process configuration of the conventional dual-stage Selexol unit is shown in Fig. 2. In this simulation, it was trialled to find the operating conditions to make a Selexol process meet the following performance targets simultaneously.

- H_2 recovery of a Selexol process: 99+%.
- Overall carbon capture efficiency: 90% (base) or 95%.
- H_2S recovery of a Selexol process: 99.99+%.
- H_2S content in the CO_2 product: less than 20 ppmv.

The CO_2 product purity can be maintained as high as 97 + mol% easily as long as all the performance targets listed above are met.

The H_2 recovery of a Selexol process is defined as:

$$H_2 \text{ recovery} = \frac{H_2 \text{ in syngas product } CO_2 \text{ absorber} - H_2 \text{ in t-syngas recycled to } H_2S \text{ concentrator}}{H_2 \text{ in main shifted syngas from mercury removal}} \quad (5)$$

It should be noted that, in the denominator of Eq. (5), the H_2 flowrate is not the flowrate of H_2 contained in the total gas stream being fed to a Selexol process, (3) in Table 2, but one in the main syngas stream, (1). This is because the H_2 in the recycle stream, (2), should not be considered as a new H_2 feed. The part of the decarbonised syngas product leaving the CO_2 absorber must be recycled to the dual-stage Selexol process as a stripping gas for enriching H_2S in the solvent. The use of syngas product as a stripping gas will be discussed in details later.

The H_2S recovery of a Selexol process is calculated by:

$$H_2S \text{ recovery} = \frac{H_2S \text{ is sour gas at } H_2S \text{ Stripper}}{H_2S \text{ in main syngas from mercury removal}} \quad (6)$$

Fig. 2 shows a schematic diagram of the conventional, integrated dual-stage Selexol process simulated in this study (Ahn et al., 2014). After the main shifted syngas stream is combined with the recycle gas from Claus plant, the gas mixture is sent at 24 °C to a H_2S absorber (20 trays) where the H_2S is preferentially absorbed into a

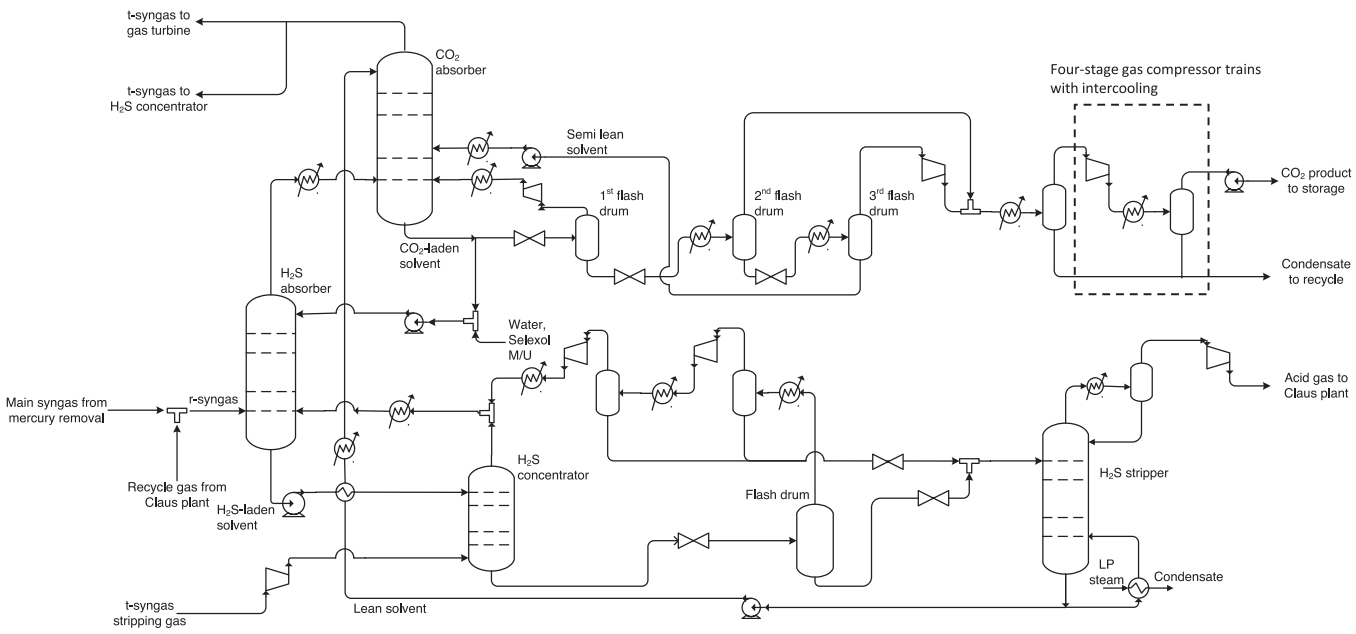

Fig. 2. Schematic diagram of an integrated dual-stage Selexol process.

CO_2-laden solvent flowing out of the bottom of a CO_2 absorber. A H_2S-laden solvent leaving the bottom of the H_2S absorber flows to a H_2S concentrator (15 trays) followed by a flash drum in order to desorb CO_2 and H_2 out of the solvent for enriching H_2S in the solvent. This is because steam stripping taking place in the H_2S stripper would regenerate Selexol solvent to an extent of being practically free of the acid gases. In other words, CO_2 as well as H_2S would be stripped off the solvent by the upflow of steam and the desorbed CO_2 and H_2S are made up of a sour gas stream on the H_2S stripper overhead. If very high carbon capture efficiency over 90% is required or the H_2S mole fraction in the sour gas needs to be maintained as high as possible, it is essential to desorb CO_2 out of the H_2S-laden solvent before the solvent is regenerated by a H_2S stripper. As gas streams generated at the H_2S enriching section also contain significant amounts of H_2S as well as CO_2 and H_2, they cannot be sent directly to the CO_2 absorber but must be recycled to the H_2S absorber for capturing H_2S from the recycle gas again.

Even though CO_2 must be desorbed preferentially over H_2S when depressurising the H_2S-laden solvent, the simple depressurisation must not be used alone for enriching H_2S since the power consumption for recycle gas compression would be costly. In this study, a H_2S concentrator operating at a high pressure is installed upstream of a flash drum in order to reduce the power consumption for recycle gas compression. Part of the treated syngas (t-syngas) leaving the top of the CO_2 absorber is used as the stripping gas for the H_2S concentrator. The selection of stripping gas is one of the crucial decision points to be made in the design of a dual-stage Selexol unit. For example, a nitrogen stream from an air separation unit may also be used instead of the t-syngas. Nitrogen can also be utilised as the stripping gas as long as the amount of nitrogen being used as the stripping gas is less than the amount of nitrogen to be used for diluting the fuel gas for combustion. Some of the stripping nitrogen gas is adsorbed by the Selexol solvent at the CO_2 absorber and subsequently they may deteriorate the CO_2 product purity. However most of the absorbed nitrogen as well as the absorbed hydrogen can be rejected out of the CO_2-laden solvent by desorption at the 1st flash drum. Therefore, the CO_2 purity can still be maintained as high as 97%. The H_2 purity of the t-syngas will be reduced from 87% to 82% due to the t-syngas being diluted by the stripping nitrogen gas. However, the t-syngas as the stripping gas at the H_2S concentrator could not be replaced with nitrogen if it was aimed to produce ultrapure hydrogen out of the H_2-enriched syngas. This is because, for producing a very high purity of H_2, the t-syngas leaving the CO_2 absorber must be sent to a H_2 purification Pressure Swing Adsorption (PSA) unit at as high a H_2 purity as possible (Luberti et al., 2014). A dilution of the H_2-enriched syngas by nitrogen would deteriorate the performance of a H_2 PSA.

If a H_2S concentrator operates at a higher pressure, the required amount of stripping gas must be greater than it would be for a H_2S concentrator operating at a lower pressure due to the difference of CO_2 partial pressure in the gas phase. The greater consumption of stripping gas gives rise to increasing power consumption for compressing the stripping gas because the stripping gas must be pressurized up to the operating pressure of the H_2S concentrator. On the contrary, the gas stream generated from the H_2S concentrator operating at a pressure higher than the pressure of the H_2S absorber can be sent directly to the H_2S absorber without having to compress it. Therefore, there is a trade-off between the two power consumptions for stripping gas compression and for recycle gas compression depending on the selection of the H_2S concentrator pressure. Given the fact that the t-syngas is already at a high pressure when produced from the CO_2 absorber, it does not have to be compressed to a great extent for its use as a stripping gas. Therefore, it is more reasonable to operate the H_2S concentrator at a pressure that is slightly higher than the H_2S absorber pressure rather than at a low pressure in order to minimize the power consumption involved in the H_2S concentrator. For the H_2S concentrator to be operated at the high pressure, the H_2S-laden solvent needs to be slightly pressurised by a pump and then fed to the H_2S concentrator. Since the extent of CO_2 removal at the H_2S concentrator is not large enough for achieving 90% carbon capture efficiency, a flash drum for further CO_2 desorption is installed to complement the H_2S concentrator. The pressure of the flash drum to determine the amount of CO_2 being desorbed was chosen so that the CO_2 mole fraction of the sour gas flowing to a Claus plant can be lower than 0.6.

The Selexol solvent must contain a small amount of water in it so that the water can be boiled off to generate steam that is used as a stripping gas in the H_2S stripper. In this study, the water content in Selexol solvent was set as 5 wt%. It is recommended that the water content in a Selexol solvent be less than 5 wt% since the viscosity of Selexol solvent increases gradually as more water is

Table 3
Key operating conditions and energy consumptions of integrated or unintegrated dual stage Selexol processes at 90% (or 95%) carbon capture efficiency.

Case	Integrated dual-stage Selexol unit (90% carbon capture)	Integrated dual-stage Selexol unit (95% carbon capture)	Unintegrated dual-stage Selexol unit (90% carbon capture)
Carbon capture efficiency [%]	90.0	95.0	90.3
CO_2 product purity [mol%]	97.2	97.6	97.3
H_2 recovery [%]	99.0	99.1	99.0
$L_{S,lean}/V_S$ (CO_2 absorber)	0.71	1.82	–
L_S/V_S (CO_2 absorber)	5.20	6.01	3.53
1st flash drum P [bar]	18.5	19.5	19.5
H_2S stripper duty [MW_{th}]	14.6	39.1	20.8
CO_2 compression power [MW_e]	32.1	33.5	30.6
Auxiliary power consumption in dual-stage Selexol units [MW_e]			
Total auxiliary power consumption	20.0	33.0	28.0
H_2S concentrator stripping gas compressor	0.14	0.14	0.13
Compressor for recycle gas from flash drum in H_2S removal section	1.00	11.1	2.72
Compressor for recycle gas from 1st flash drum	0.74	0.65	0.57
H_2S-laden solvent pump	0.10	0.26	0.15
CO_2-laden solvent pump	0.04	0.10	0.0
Lean solvent pump	2.24	6.72	3.84
Semi-lean solvent pump	15.6	13.8	20.4
Sour gas compressor	0.20	0.22	0.22

added (Macjannett, 2012). The H_2S stripper driven by low pressure steam can regenerate the solvent completely, i.e. the lean solvent contains practically neither CO_2 nor H_2S.

The gas stream leaving the H_2S absorber is fed to the CO_2 absorber (20 trays) at 24 °C. There are two different solvents being utilised for capturing CO_2 at the CO_2 absorber. One is a lean solvent coming from the H_2S stripper which is sent to the top of CO_2 absorber. The other is a semi-lean solvent from the last stage of flash drums that enters the tray (tray 16) located at the 1/4th of the column from the bottom. The CO_2-laden solvent leaving the CO_2 absorber is split into two streams: one is sent to three successive flash drums operating at high, medium, and low pressures where the CO_2-laden solvent becomes regenerated by stepwise depressurisation over the flash drums. The other is directed to the H_2S absorber for capturing H_2S from the gas feed in order to prevent the gas stream from carrying H_2S to the CO_2 absorber. The flowrate of the CO_2-laden solvent flowing to the H_2S absorber was determined so that the dual-stage Selexol unit can achieve 99.99+% of H_2S capture rate, eventually resulting in less than 20 ppmv H_2S in the CO_2 product.

The CO_2-laden solvent contains significant amount of hydrogen as well as CO_2 even though the solubility of H_2 relative to CO_2 is only 0.013 as listed in Table 1. In order to achieve the very high H_2 recovery of 99%, most hydrogen contained in the CO_2-laden solvent must be recovered and sent back to the CO_2 absorber. The 1st flash drum plays a role in recovering H_2 from the CO_2-laden solvent. Without the 1st flash drum, most hydrogen absorbed by the solvent would end up in the CO_2 product, leading to both unsatisfactory H_2 recovery and CO_2 product purity. In this study, the maximum pressure of the 1st flash drum for meeting the H_2 recovery target was found to be 18.5 bar. The gas stream from the 1st flash drum having around 57 mol% H_2 is recycled to the CO_2 absorber after compression.

The H_2-depleted solvent after the 1st flash drum is sent to the 2nd and 3rd flash drums in series in order to recover CO_2 from the solvent. The pressure of the 3rd flash drum was set as a pressure close to ambient pressure in order to maximise the CO_2 working capacity. The 2nd flash drum was designed to operate at 3.45 bar since the CO_2 product at the 3rd flash drum is compressed up to the pressure of the CO_2 product at the 2nd flash drum with a compression ratio of around 3. The CO_2 product compression section was configured such that, after the first stage of compression, it has a four-stage compression trains with intercooling and finally one pump for pressurising the liquid-like CO_2 product up to 150 bar (Ahn et al., 2013). The temperature of the CO_2-laden solvent keeps decreasing in the course of depressurisation over the flash drums due to the endothermic heat of desorption. If the solvent temperature decreased below 25 °C after its depressurisation, it was heated up to 25 °C before entering the next flash drum assuming that there would be plenty of waste heat sources available around the site for such a heating.

As shown in Table 3, the power consumption relating to auxiliary units and CO_2 compression amount to 20.0 MW_e and 32.1 MW_e respectively that are very close to 18.7 MW_e and 30.2 MW_e that DOE NETL (2010) reported in the Case 6. On the contrary, the heat duty at the H_2S stripper was estimated to be around 14.6 MW_{th} that is less than half of the DOE number (35.3 MW_{th}). This discrepancy can be explained in part by inaccuracy of our solubility model estimating greater H_2S solubility in Selexol than those in the literature (see Fig. 1). On the other hand, DOE might assign to the heat duty of the H_2S stripper a plentiful safety margin for operational flexibility or oversize it in preparation for processing high-sulphur coals instead of the design coal.

4. Unintegrated dual-stage Selexol process

It is conceivable to modify the dual-stage Selexol process to a simpler configuration where the two solvent cycles for H_2S and CO_2 removals are independent of each other, hereinafter called unintegrated dual-stage Selexol process. As shown in Fig. 3, the CO_2 absorber operates with only the semi-lean solvent that is produced by three successive flash drums without having any lean solvent originating from the H_2S absorber. The H_2S absorber does not operate with a semi-lean solvent flowing from the CO_2 absorber but it does with a lean solvent. Given the fact that significant change was made to both H_2S and CO_2 absorbers, it is interesting to see if the unintegrated process can still achieve the targets set out in this study and to evaluate the energy consumption at the operating conditions meeting the targets.

Any new unit was not deployed in addition to what are used for configuring the integrated dual-stage Selexol process but the connections of several streams were altered so as to configure the two independent solvent cycles for H_2S and CO_2 removals. The configuration requires that the semi-lean solvent from the 3rd flash drum is fed to the top of the CO_2 absorber instead of its middle since

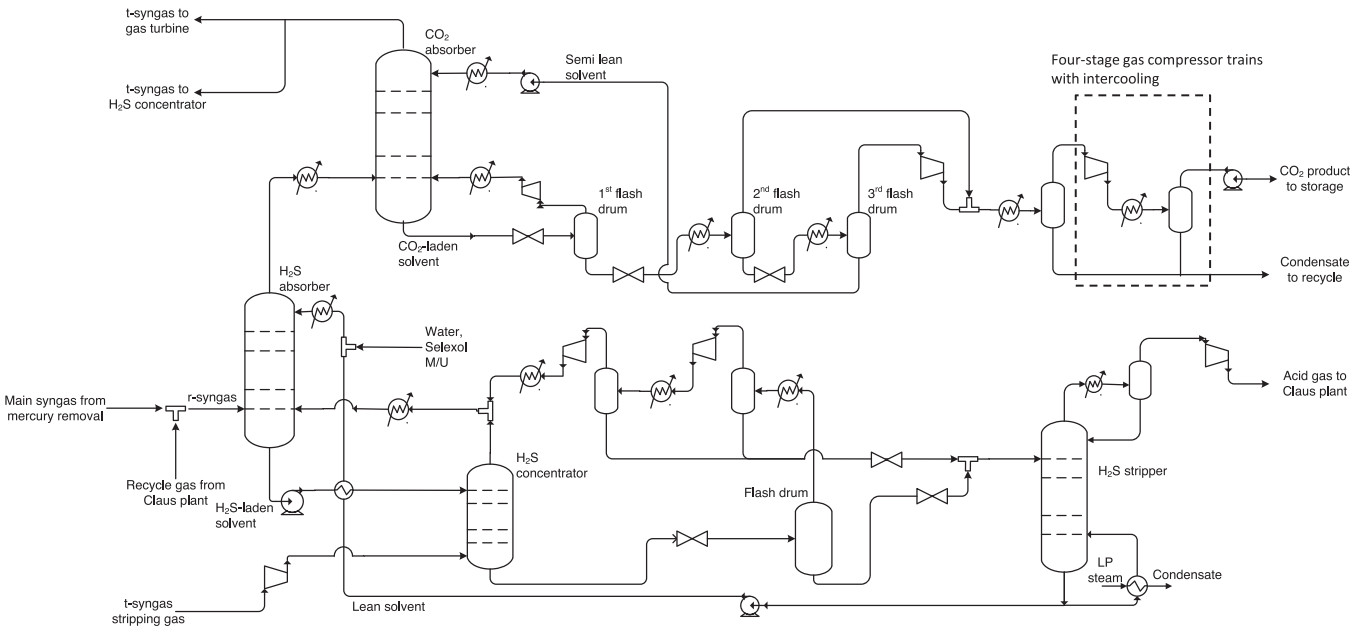

Fig. 3. Schematic diagram of an unintegrated dual-stage Selexol unit.

there is no lean solvent available for the CO_2 absorber. Now that the semi-lean solvent for the CO_2 absorber is not involved in any steam stripping, it does not have to contain any water. In other words, the CO_2 removal cycle can be initiated with a pure, dehydrated Selexol solvent even though some water vapor in the gas stream will be absorbed into the circulating Selexol solvent due to its high water solubility.

Fig. 4shows the operating and equilibrium lines of the CO_2 absorber at the unintegrated dual-stage Selexol process at various solvent flowrates. The equilibrium lines were plotted with an assumption of a linear change of temperature along the CO_2 absorber between the two temperatures at both ends obtained in the simulation. Given the fact that Selexol has a negligible vapor pressure and CO_2 is only one major gas component involved in reaction taking place in the CO_2 absorber, it is useful to plot the operating lines in terms of molar ratio instead of molar fraction as follows:

$$Y = \frac{L_{Sc}}{V_{Sc}}X + \frac{V_{Sc}Y_c - L_{Sc}X_c}{V_{Sc}} \quad (7)$$

where X and Y are the molar ratios in the liquid and gas phases, i.e., $\frac{x_{CO_2}}{(1-x_{CO_2})}$ and $\frac{y_{CO_2}}{(1-y_{CO_2})}$, L_S and V_S are the total molar flowrates except for CO_2 in the liquid and gas phases, i.e., $L(1-x_{CO_2})$ and $V(1-y_{CO_2})$. Subscript c denotes an arbitrary axial position of the CO_2 absorber.

Strictly speaking, the slope of operating line, L_{Sc}/V_{Sc}, cannot be kept constant along the CO_2 absorber since other gaseous components, such as CO, CH_4 and H_2can also be absorbed. Nevertheless a change of the slope along the CO_2 absorber can be practically neglected since CO and CH_4 exist in the gas feed much less than CO_2 and the solubilities of CO, CH_4 and H_2 relative to CO_2 are significantly low. In this study, therefore, it was assumed that the operating line of Eq. (7) would be linear along the CO_2 absorber. Based on the assumption, each operating line could be constructed with the CO_2 mole fractions in the gas and liquid phases and the gas and liquid molar flowrate at a position of CO_2 absorber. This assumption was validated given the fact that the operating line being constructed with the information at only one end of the CO_2 absorber can estimate the CO_2 molar ratio at the other end as shown in Fig. 4. This observation also indicates that our CO_2 absorber simulations using UniSim were sufficiently accurate since the mass balance around the CO_2 absorber was closed.

As an initial trial, the unintegrated dual-stage Selexol process was simulated with a seme-lean flowrate at $L_S/V_S = 2.54$ and its carbon capture efficiency was only 78.7%. (Note that subscript c was omitted since the slope is effectively independent of the axial position of the CO_2 absorber.) But it was foreseen that the capture efficiency could be improved further by increasing the semi-lean solvent flowrate since the operating line was away from the equilibrium line at $L_S/V_S = 2.54$ as shown in Fig. 4. As expected, the carbon capture efficiency was increased up to 90.3% by increasing L_S/V_S up to 3.53.

However, it should be noted that there is little room to improve the carbon capture efficiency further above 90% at the unintegrated process. At $L_S/V_S = 3.53$, the operating line was already very close to its associated equilibrium line, i.e., a pinch point was almost reached at the top of the CO_2 absorber. Therefore, it must be very difficult to increase the carbon capture efficiency over 90% however much the solvent flowrate would be increased above $L_S/V_S = 3.53$. At $L_S/V_S = 18.7$ that is more than five times greater than that for the 90% carbon capture case, the carbon capture efficiency was only 91.8%. In other words, the increase of solvent flowrate cannot decrease the CO_2 molar fraction of the gas stream leaving the CO_2 absorber but decrease the CO_2 molar fraction of rich solvent at the bottom. Additionally, the increasing solvent flow absorbs more hydrogen from the syngas, so the H_2 recovery would be reduced well below 99% without decreasing the 1st flash drum pressure for desorbing more H_2 from the CO_2-laden solvent.

The power consumption at the unintegrated dual-stage Selexol unit was increased by 40% against the level at the integrated process under the condition of 90% carbon capture. This is mainly due to it requiring higher mass flowrate of the circulating semi-lean solvent than the integrated process in order to make up for reduced CO_2 working capacity of the solvent, leading to greater power consumption in semi-lean solvent pump.

5. 95% Carbon capture efficiency

From the simulation study on the unintegrated process, it can be concluded that it would be very difficult to achieve 95% carbon capture efficiency with a CO_2 absorber operating with semi-lean solvent only. The pinch point formed at the top end of the CO_2

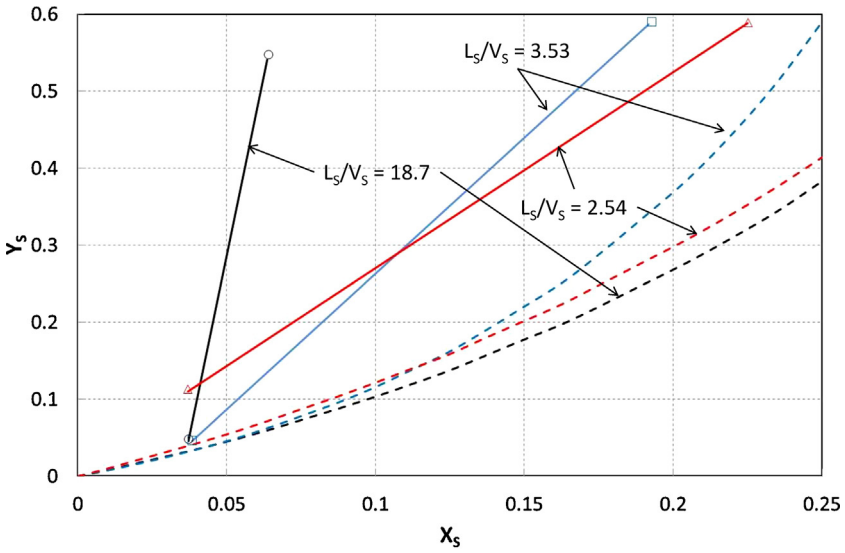

Fig. 4. Operating and equilibrium lines of CO_2 absorbers of unintegrated dual-stage Selexol process at various solvent flowrates. (solid lines: operating lines, broken lines:equilibrium lines, symbols: UniSim simulation results).

absorber must be eliminated in order to achieve as high as 95% carbon capture efficiency.

One obvious way of avoiding such a pinch point at the top end is to feed a lean solvent, i.e., CO_2-free solvent, to the top end in addition to a semi-lean solvent entering the middle of the absorber just as the CO_2 absorber of the conventional integrated dual-stage Selexol process is configured. Fig. 5 shows the operating and equilibrium lines of the CO_2 absorber at the integrated solvent cycle at 90% carbon capture efficiency. The addition of CO_2-free lean solvent flow could make the operating line away from the equilibrium line by moving the CO_2 mole fraction in the liquid phase at the top end to effectively zero. Therefore the integrated dual-stage Selexol process paves a way for achieving a carbon capture efficiency higher than 90%.

It was attempted to improve the carbon capture efficiency by 5% point in order to achieve 95% carbon capture efficiency with the integrated process. The substantial increase in the carbon capture efficiency may be made by increasing only the semi-lean solvent flowrate with the lean solvent flowrate kept constant. But it would be easier to achieve the 5% increase by increasing the lean solvent flowrate than the semi-lean solvent flowrate since the use of the lean solvent is essential to overcome the pinch point at the top end. Therefore it was trialled to increase the lean solvent flowrate as much as possible in the first place and then adjust the semi-lean solvent flowrate to achieve 95% carbon capture.

However there exists a maximum beyond which the lean solvent flowrate cannot be increased. In order to increase the lean solvent flowrate to the CO_2 absorber, the flowrate of the CO_2-laden solvent flowing to the H_2S absorber must be increased. This is because the CO_2-laden solvent flowing to the H_2S absorber will be regenerated at the H_2S stripper and then returned to the CO_2 absorber as a lean solvent. The more CO_2-laden solvent flows to the H_2S absorber, the greater amount of CO_2 it also conveys from the CO_2 absorber to the H_2S absorber. Consequently, the flash drum

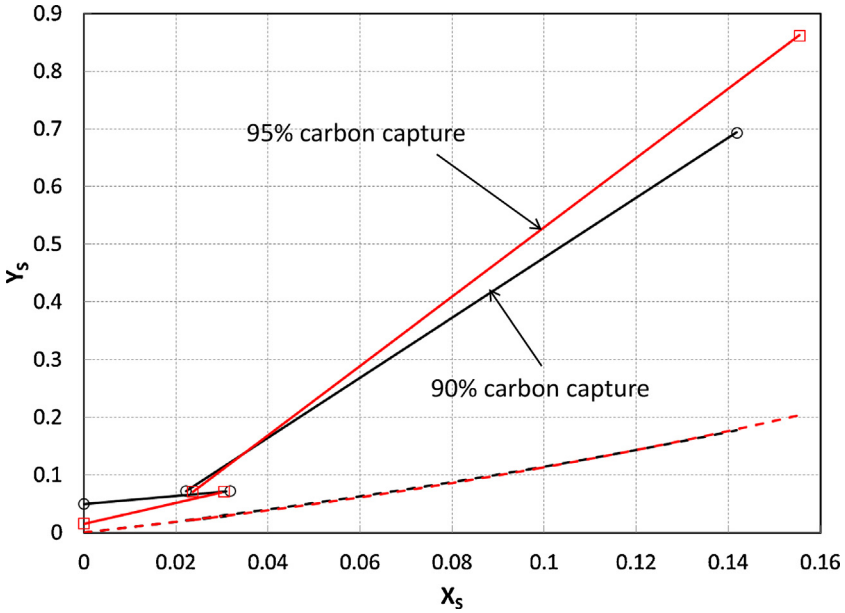

Fig. 5. Operating and equilibrium lines of CO_2 absorbers of integrated dual-stage Selexol process at 90% and 95% carbon capture rates (solid line: operating lines, broken lines: equilibrium lines, symbols: UniSim simulation results).

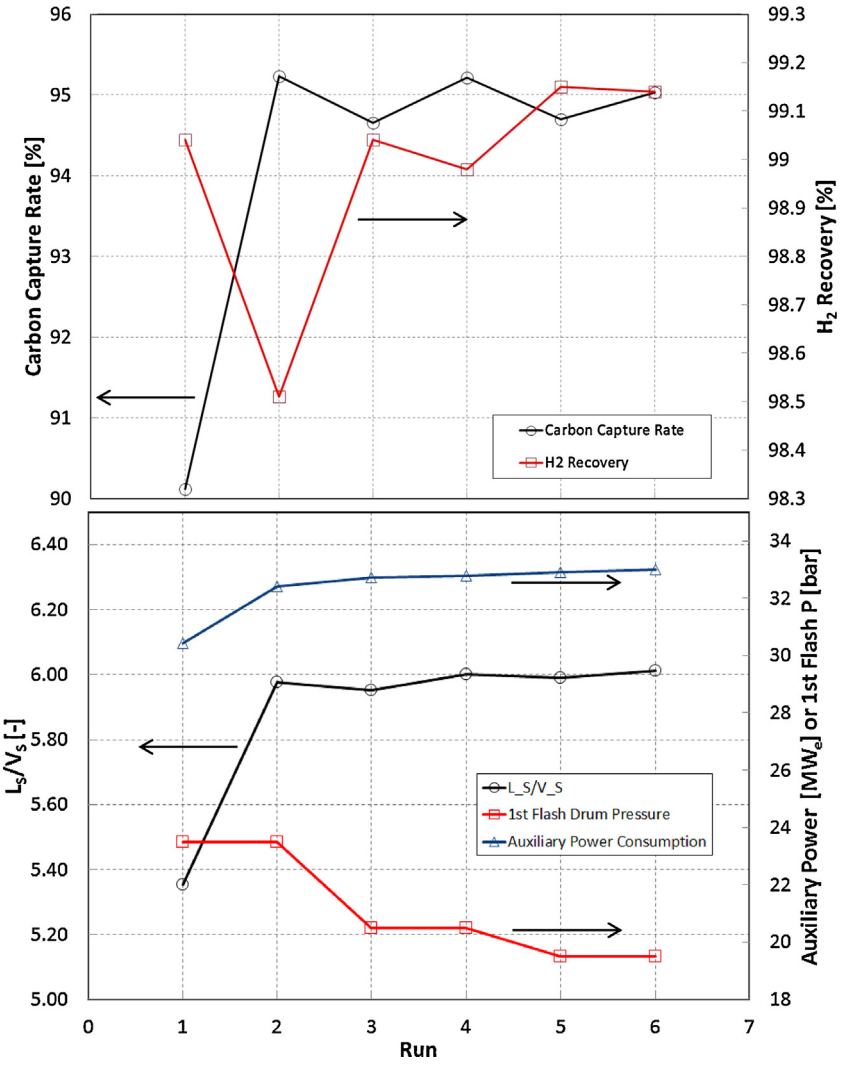

Fig. 6. Change of performance and operating conditions over the simulation runs of an integrated dual-stage Selexol process for increasing the carbon capture rate from 90% to 95%.

for enriching the H_2S in the solvent needs to operate at a lower pressure in order to send the CO_2 carried by the solvent back to the CO_2 absorber. However the flash drum pressure must be higher than the operating pressure of the H_2S stripper close to ambient pressure. In this study, the maximum lean solvent flowrate that is allowed at the minimum flash drum pressure of 150 kPa was around 1.82 of L_{S_lean}/V_S as listed in Table 3.

In the first place, the existing simulation for integrated process at 90% carbon capture efficiency (old 90% case) was modified to new 90% case with the higher lean solvent flowrate (Run 1 in Fig. 6). At Run 1, it was expected that the semi-lean solvent flowrate would be lowered thanks to the increased lean solvent flowrate. Contrary to our expectation, the L_S/V_S is still as high as 5.35 (Fig. 6) that is rather higher than 5.20 in the old 90% case (see Table 3). This can be explained by more CO_2 being required to be captured in the CO_2 absorber of the new 90% case to achieve the target of 90% carbon capture efficiency in overall because the amount of CO_2 being sent to the H_2S absorber was larger in the new 90% case than in the old 90% case. Therefore, more CO_2 was actually captured at the CO_2 absorber in the new 90% case than in the old 90% case but the CO_2 recovery were almost the same in the two cases, i.e., 90% carbon capture efficiency, since more captured CO_2 was carried by the increased CO_2-laden solvent flow to the H_2S absorber. It should be noted that, in case of the new 90% case, the 1st flash drum could be operated at 23.5 bar that is higher than 18.5 bar of the old 90% case. The increase of the 1st flash drum pressure in modifying the old 90% case to a new 90% case seems far-fetched in that the required amount of the H_2 to be desorbed from the CO_2-laden solvent for achieving the H_2 recovery target must be greater at the new 90% case than at the old 90% case. This is because the total solvent flowrate entering the CO_2 absorber was larger at the new 90% case. Nevertheless a less amount of H_2 needs to be desorbed at the 1st flash drum at the new 90% case because the increased CO_2-laden solvent flow to the H_2S absorber also carries greater amount of H_2 that is subsequently desorbed at both H_2S concentrator and flash drum and eventually recycled back to the CO_2 absorber.

As the lean solvent flowrate at new 90% case was already at its maximum, it could not be increased further. Therefore the carbon capture efficiency was increased up to 95% by increasing the total solvent flowrate from 5.35 to 5.99 of L_S/V_S (Run 2). Again, the increase of the total solvent flowrate was made by increasing only the semi-lean flowrate. However, the H_2 recovery was decreased from 99.0% to 98.5% due to more hydrogen being sent to the CO_2 product stream. In Run 3, the 1st flash drum pressure was reduced to 20.5 bar from 23.5 bar to recover more hydrogen and recycle it to the CO_2 absorber. As more gas stream including CO_2 was recycled to the CO_2 absorber, the carbon capture efficiency dropped below 95%, so the semi-lean solvent flowrate needed to be increased again (Run 4). At Run 5, the 1st flash drum pressure was reduced to 19.5 bar to maintain the H_2 recovery over 99%. Finally, Run 6 could meet

targets of both 95% CO_2 capture rate and 99% H_2 recovery rate by changing the operating conditions of the integrated process without having to add any other equipment. The operating conditions and simulation results at Run 6 are presented in Table 3.

As a result, the total auxiliary power consumption was increased by 65% only for increasing the carbon capture efficiency by 5% point. The significant increase of power consumption is relating to the increasing flowrate of CO_2-laden solvent flowing to the H_2S absorber giving rise to greater power consumption in compressing the recycle gas being desorbed from the flash drum and in pressurising the lean solvent.

In Fig. 5, the operating and equilibrium lines around the CO_2 absorber at the integrated dual-stage Selexol process at 95% carbon capture efficiency was added. As more CO_2 is transferred from the CO_2 removal section to the H_2S removal section with the increased CO_2-laden solvent flowrate, the gas stream flowing to the CO_2 absorber has a higher CO_2 mole fraction resulting in increasing Y_S at the bottom end. Fig. 5 demonstrates that it is essential to have a sharper slope of the operating line in the upper section of the CO_2 absorber in order to achieve as high as 95% carbon capture efficiency.

6. Conclusions

A conventional dual-stage Selexol process for CO_2 and H_2S removal from an exemplary dry-coal fed gasifier IGCC power plant (DOE NETL, 2010) was simulated. The solubilities of syngas components in Selexol were predicted by Henry's Law in combination with Peng-Robinson EOS for taking a non-ideal behavior in the gas phase into account.

It was demonstrated by simulation that both integrated and unintegrated dual-stage Selexol processes could achieve 90% carbon capture efficiency. While the carbon capture efficiency in the integrated process could be enhanced up to 95% by changing the operating conditions and spending more energy, it was not possible to do so in case of the unintegrated process. This is because, in the CO_2 absorber of the unintegrated process, there is not a lean solvent input that is essential to avoid a pinch point at the top end of the CO_2 absorber.

The power consumption of the integrated dual-stage Selexol process for 95% carbon capture was 65% greater than the level at 90% capture case. In this study a strategy was taken to increase the lean solvent flowrate for CO_2 absorber to the maximum and then adjust the semi-lean solvent flowrate. Meanwhile, there may be a chance to reduce the power consumption at 95% capture case by optimising the flowrate ratio of lean solvent to semi-lean solvent.

Acknowledgements

We would like to express our gratitude for the financial support from EPSRC (Grants No.: EP/F034520/1, EP/G062129/1, and EP/J018198/1), KETEP (Grant No.: 2011-8510020030) and ETI-funded Next Generation Capture Technology (NGCT) project led by Costain.

References

Ahn, H., Luberti, M., Liu, Z., Brandani, S., 2013. Process configuration studies of the amine capture process for coal-fired power plants. Int. J Greenh. Gas Control 16, 29–40.
Ahn, H., Kapetaki, Z., Brandani, P., Brandani, S., 2014. Process simulation of a dual-stage Selexol unit for pre-combustion carbon capture at an IGCC power plant. Energy Procedia 63, 1751–1755.
Bhattacharyya, D., Turton, R., Zitney, S.E., 2011. Steady-state simulation and optimization of an integrated gasification combined cycle power plant with CO_2 capture. Ind. Eng. Chem. Res. 50, 1674–1690.
Bucklin, R.W., Schendel, R.L., 1984. Comparison of fluor solvent and Selexol processes. Energy Progress 4, 137–142.
Burr, B., Lyddon, L., 2008. A comparison of physical solvents for acid gas removal. 87th Annual GPA Convention.
Cai, H.-Y., Shaw, J.M., Chung, K.H., 2001. Hydrogen solubility measurements in heavy oil and bitumen cuts. Fuel 80, 1055–1063.
Chen, C., Rubin, E.S., 2009. CO_2 control technology effects on IGCC plant performance and cost. Energy Policy 37 (3), 915–924.
Chiesa, P., Consonni, S., 1999. Shift reactors and physical absorption for low-CO_2 emission IGCCs. J. Eng. Gas TurbinesPower 121 (2), 295–305.
Committee on Climate Change, 2013. Reducing the UK's carbon footprint and managing competitiveness risks.
Confidential Company Research Report, 1979. Gas absorption in Selexol, (Available in DETHERM database, http://detherm.cds.rsc.org/index.php).
Cormos, C.-C., Agachi, P.S., 2012. Integrated assessment of carbon capture and storage technologies in coal-based power generation using CAPE tools. In: Proceedings of the 22nd European Symposium on Computer Aided Process Engineering, London, pp. 56–60.
Davison, J., Bressan, L., 2003. Coal power plants with CO_2 capture: the IGCC Option. Gasification Technologies.
DOE NETL, 2002. Advanced fossil power systems comparisons study.
DOE NETL, 2010. Cost and performance baseline for fossil energy plants volume 1: bituminous coal and natural gas to electricity Rev. 2. 2010/1397.
Doctor, R.D., Molburg, J.C., Thimmapuram, P.R., 1996. KRW oxygen-blown gasification combined cycle: carbon dioxide recovery, transport, and disposal. ANL/ESD-34.
Kapetaki, Z., Ahn, H., Brandani, S., 2013. Detailed process simulation of pre-combustion IGCC plants using coal-slurry and dry coal gasifiers. Energy Procedia 37, 2196–2203.
Kohl, A.L., Nielsen, R.B., 1997. Gas Purification. Gulf Professional Publishing.
Luberti, M., Friedrich, D., Brandani, S., Ahn, H., 2014. Design of a H_2 PSA for cogeneration of ultrapure hydrogen and power at an advanced integrated gasification combined cycle with pre-combustion capture. Adsorption 20, 511–524.
Macjannett, J., 2012. Using physical solvent in multiple applications, (http://www.digitalrefining.com/article/1000359,Using_physical_solvent_in_multiple_applications_.html#.UrHd751FCUk) as of 29/11/2014.
O'Keefe, L.F., Griffiths, J., Weissman, R.C., De Puy, R.A., Nathan, E., Wainwright, J.M., 2002. A single IGCC design for variable CO_2 capture. In: 5th European Gasification Conference, Noordwijk, The Netherlands.
Padurean, A., Cormos, C.-C., Agachi, P.-S., 2012. Pre-combustion carbon dioxide capture by gas–liquid absorption for integrated gasification combined cycle power plants. Int. J. Greenh. Gas Control 7, 1–11.
Robinson, P.J., Luyben, W.L., 2010. Integrated gasification combined cycle dynamic model: H_2S absorption/stripping, water–gas shift reactors, and CO_2 absorption/stripping. Ind. Eng. Chem. Res. 49 (10), 4766–4781.
Rubin, E.S., Chen, C., Rao, A.B., 2007. Cost and performance of fossil fuel power plants with CO_2 capture and storage. Energy Policy 35 (9), 4444–4454.
Saajanlehto, M., Uusi-Kyyny, P., Alopaeus, V., 2014. Hydrogen solubility in heavy oil systems: experiments and modeling. Fuel 137, 393–404.
Sweny, J.W., Valentine, J.P., 1970. Physical solvent stars in gas treatment/purification. Chem. Eng. 77 (19), 54–56.
UniSim Design, 2013. Simulation Basis Reference Guide. Honeywell, pp. A35–A37.
Wang, Y., Ling, K., Shen, J., Zhu, T., 2013. A determination and correlation on the solubility of hydrogen in Shenhua coal liquiefied oils at high pressures. Energy Sour. Part A 35, 2002–2009.
Xu, Y., Schutte, R.P., Hepler, L.G., 1992. Solubilities of carbon dioxide: hydrogen sulfide and sulfur dioxide in physical solvents. Can. J. Chem. Eng. 70, 569–573.
Zhang, D.D., Ng, H.J., Veldman, R., 1999. Modelling of acid gas treating AGR physical solvent. Proceedings of the 78th GPA Annual Convention 78, 41244.